The performances of the upgraded surface detector stations of AugerPrime

Fabio Convenga^{a,b,*} **for the Pierre Auger Collaboration**^{c}

^{a}*Università dell'Aquila*

^{b}*INFN Laboratori Nazionali del Gran Sasso, Assergi (L'Aquila), Italy*

^{c}*Observatorio Pierre Auger, Av. San Martín Norte 304, 5613 Malargüe, Argentina*
   Full author list: https://www.auger.org/archive/authors_icrc_2023.html

   E-mail: spokespersons@auger.org

The surface detector of the Pierre Auger Observatory is an array of 1,600 stations using a water Cherenkov detector (WCD) for particle detection. The array is undergoing a major upgrade known as AugerPrime that involves adding scintillator surface detectors (SSDs) and radio antennas to the existing WCDs. Each WCD is also equipped with a smaller photomultiplier tube added to the original ones. As part of the upgrade, underground muon detectors are being installed in an area with a higher density of surface detector stations. AugerPrime required the development of new electronics to process the signals from all the new detectors and handle a higher sampling rate, a more precise GPS receiver, an extended dynamic range, higher processing capacity, and improved monitoring systems and memory. The deployment of the SSDs on top of each surface detector station is currently completed together with the deployment of the new electronics. This contribution will present the first data from the upgraded stations, emphasizing the performances of the SSDs and the new electronics.

---

*Speaker

Figure 1: (Left) A surface station upgraded with AugerPrime detectors. Visible are the SSD on top of the WCD, together with the radio detector, which is the antenna on top of the SSD. The UUB is placed under the dome (red annotation), which is visible between the top of the WCD and the bottom of the SSD. (Right) Photo of a UUB, it when installed under the dome is primarily inserted in a metal shielding for protection.

1. Introduction

The Pierre Auger Observatory, situated near the city of Malargüe in the Pampas region of Argentina, spans an area of $3000\,\text{km}^2$ and comprises 1600 water Cherenkov detector (WCD) surface stations arranged on a triangular grid array with 1500 m spacing (SD-1500) [1]. Additionally, for lower energy measurements, two nested arrays with the same type of surface station are used in an infilled zone with a spacing of 750 m (SD-750) and 433 m (SD-433)[2]. Four fluorescence detector (FD) sites overlook the array, each equipped with six telescopes, providing a field of view of $30° \times 30°$ in both azimuth and elevation. Three additional telescopes pointing at higher elevations (HEAT) are located close one of the FD sites to detect lower energy showers.

Over its two decades of operation, the Pierre Auger Observatory has significantly contributed to ultra-high energy cosmic rays (UHECRs) research. In 2015, the Auger Collaboration decided to undertake a substantial upgrade known as AugerPrime [3] to investigate UHECR composition and hadronic interaction effects at the highest energies. The AugerPrime upgrade involves the addition of a scintillator-based surface detector (SSD) [4] and a radio detector (RD) [5] to each WCD surface station. This configuration will improve the discrimination of the muonic and electromagnetic components of the shower based on the distinct responses of each detector. Furthermore, the SSD and RD offer complementary coverage angles, with the SSD optimized for more vertical showers and the RD optimized for showers with higher zenith angles. As part of AugerPrime, in each surface station, a small, 1-inch photomultiplier (sPMT) [6] has been added to the three existing large PMTs (LPMTs) to extend the dynamic range. Also, underground muon detectors (UMDs) [7] are being buried in the infill zone to measure the muon component directly. In Fig. 1 an upgraded station is shown on the left with the SSD and RD installed on the top.

The surface detector electronics have been also upgraded [8] to acquire and manage the new detectors. The previous electronics, known as Unified Board (UB), is replaced by a new board called Upgraded Unified Board (UUB). The UUB, in addition to WCD, supports the SSD, RD, UMD, and the sPMT, maintains backward compatibility with the current dataset and implements

additional trigger types. A photo of UUB is shown on the right panel of Fig. 1.

2. The Upgraded Unified Board

The UUB has been designed to process the new signals from the upgraded surface station. The UUB features a new analog-to-digital converter (ADC) with 120 MHz sampling (instead of the UB's 40 MHz) and 12-bit accuracy.

The board's core is a Xilinx Zynq7020 system-on-chip, an embedded system between an ARM processor and an FPGA. The firmware implements various digital functions such as the ADC reading, the triggers generation, and the interfaces to the LED flashers, GPS receivers, and memories. The UB trigger logic has been ported to the UUB FPGA. To not interfere with the data taking during the deployment of the UUBs, the ADC traces of the three WCD PMTs are digitally filtered and downsampled to reproduce the previous trigger characteristics. However, the 120 MHz full bandwidth ADC traces are transmitted and analyzed. Additionally, the enhanced processing capabilities of the UUB FPGA allow for the implementation of new trigger types, including combined SSD and WCD triggers acting on the full bandwidth ADC traces.

The UUB utilizes the Xilinx PetaLinux operating system, which runs on the ARM processor. The local station data acquisition (LSDAQ) software [9] installed on the UUB handles high-level functions such as data management and radio communication.

The detector synchronization is done by tracking the local 120 MHz clock variations relative to the GPS 1 PPS signal. For the upgraded electronics, the Synergy SSR-6TF timing GPS receivers were chosen. The FPGA, through the time-tagging module, manages the GPS and the data timing in an entirely consistent way with the one designed for the UB. The verification of the timing performances of GPS SSR-6TF receivers was done by using a synchronization cable to send timing signals between two closely positioned (≈ 20 m) upgraded stations. With this method, a timing accuracy of about 5 ns was obtained, a result consistent with the laboratory measurements and the timing granularity as implemented on the UUB.

The ADCs at the front-end of the UUB receive signals from various components: the four photomultipliers that detect Cherenkov light from the WCD (the sPMT and the 3 LPMTs) and the PMT that collects light from the SSD. The LPMTs and SSD PMT signals are divided into four high-gain and four low-gain signals, respectively. The gain-ratio is set by the electronics design to be 32 in the case of LPMT channels and 128 in the case of SSD PMT channel to allow for an extension of the dynamic range up to 20,000 MIP (minimum-ionizing particle) to match the increased dynamic range of the WCD due to the introduction of the sPMT. The gain ratios were subsequently measured in the laboratory, obtaining a value of 32.2 with a standard deviation of 0.3 for the LPMT channels, and a value of 126.7 with a standard deviation of 1.3 for the SSD PMT channel (as shown in Fig. 2)

3. Calibration

The signals in the WCD are quantified in terms of the equivalent charge produced by a vertical-centered through-going muon, commonly referred to as VEM (vertical-equivalent muon)[10]. The SSD signals, similarly, are expressed in units of the mean signal charge produced by a MIP.
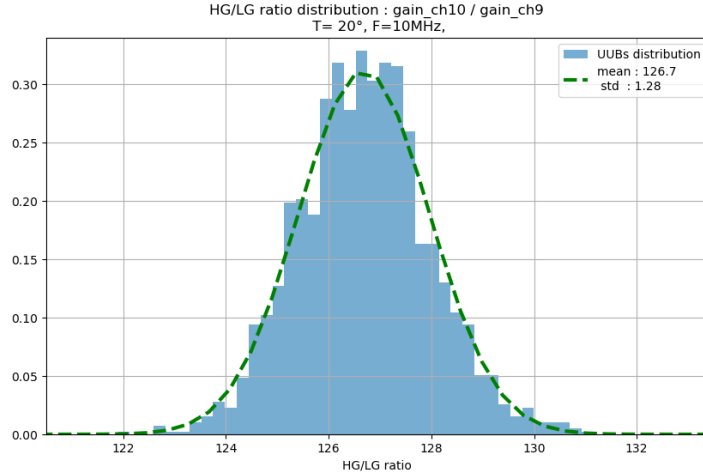
Figure 2: Distribution of the gain ratio for the channel hosting the SSD PMT in UUB measured in the laboratory during the boards testing.

Atmospheric muons passing through the detector serve as a reference for determining the value of 1 VEM and 1 MIP in ADC counts. However, since vertical-centered through-going muons cannot be specifically selected, the charge spectra of omnidirectional muons, referred to as calibration histograms, are continuously collected and employed to estimate calibration units.

Examples of calibration histograms from an upgraded station are shown in Fig. 3. The distributions have two characteristic peaks: the first peak is caused by a convolution of low-energy electromagnetic particle signals, while the second peak is due to omnidirectional through-going muons. By fitting the position of the second peak and using pre-measured conversion factors to convert the value from omnidirectional to vertical, the VEM charge is finally determined. The MIP charge is obtained by fitting the second peak position in the calibration charge histogram from SSD and using a conversion factor based on simulations. These histograms are sent to the central data acquisition system (CDAS) as part of the event and are used in the offline event reconstruction to convert raw traces into VEM and MIP units.

The ageing of the observatory detectors has an impact on the calibration histograms over time. The ageing increases the attenuation of light in WCDs, which causes the second peak due to muons to merge into the electromagnetic peak of the calibration histograms. In this way, the two peaks are not easily distinguishable, and a fit of the second one to assess the VEM is more difficult. By requiring a coincidence between the WCD and SSD detectors, a calibration histogram can be produced in which the contribution of the electromagnetic background is suppressed and the second peak is easier to fit. The impact and performances of this calibration method are described in [11].

Due to its size, the direct calibration of the sPMT with muons is not possible. However, by selecting local low-energy showers, the sPMT is cross-calibrated with the LPMTs. In this way, the conversion factor β from the collected charge measured in ADC counts into a signal expressed in VEM is obtained. With the sPMT the dynamic range of the WCD is extended up to 20,000 VEM allowing a measurement of signals down to about 250 m from the shower core in combination with the SSD. Besides, the good correlation between the calibrated WCD and SSD signals shown in ref.
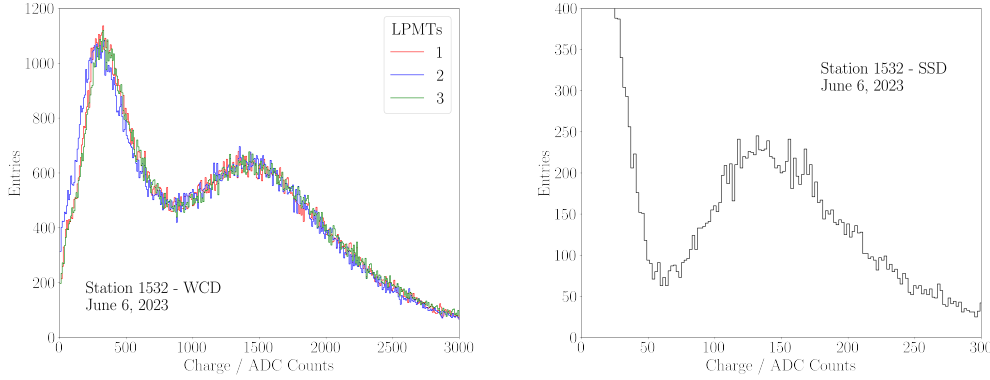
Figure 3: Example of calibration histograms of an upgraded station. (Left) The histograms of the three LPMTs. (Right) The calibration histogram of the SSD.

[6], thanks to the extended dynamic range, clearly demonstrates the validity of the two independent calibrations.

4. Status and Performances

The deployment in the array of new detectors and electronics is well advanced. The deployments of SSDs, sPMTs and UUBs in the array has been successfully completed in all accessible areas in June 2023. The deployments of RDs and UMDs are still ongoing.

During the deployment of the new electronics, data acquisition was not interrupted, and the central data acquisition software (CDAS) and data analysis pipelines were updated for AugerPrime. The acquired data was continuously monitored and analyzed to assess the long-term performances of the detection stations. The subset of parameters monitored during the deployment includes the RMS of the baseline of the ADC signal as an estimator of the noise of the electronics, the VEM charge, the MIP charge, and the β factor to assess the setting of each PMT.

The environment to which the surface stations are exposed is hostile. The terrain is changeable over $3000\,\mathrm{km^2}$ of the array, and some detectors have to cope with corrosive air of high salinity, while others have to deal with the dusty air of sandy soil. In addition, the array area is subject to strong winds and severe thunderstorms that can have lightning strikes that interfere with the electronics. At $1400\,\mathrm{m}$ altitude and with clear skies, day-night temperature variations often exceed $20\,^\circ\mathrm{C}$, this causes fluctuating daily behavior of performance parameters due to temperature sensitivity of PMTs. To cope with these variations and to keep the array as homogeneous as possible, the LSDAQ software [9] handles these effects by operating an online calibration that defines a moving threshold depending on the rate measured on the LPMTs.

The baseline RMS values of the high-gain channel for the three LMPTs are shown in the left panel of Fig. 4. The distribution in particular shows the mean RMS value per station and is made for all upgraded stations in the week following the end of the deployment in SD-1500. It shows that the noise of the high-gain channel is in general less than 2 ADC counts, meeting the design
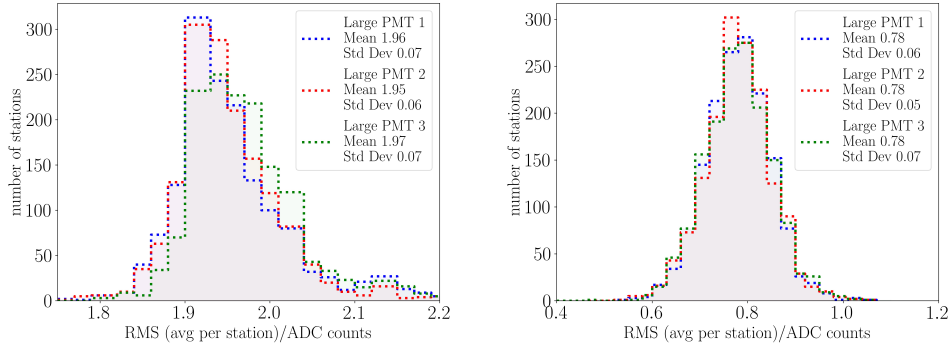
Figure 4: The mean baseline RMS of the LPMTs high-gain (Left) and low-gain (Right) measured on all upgraded stations in early July 2023.
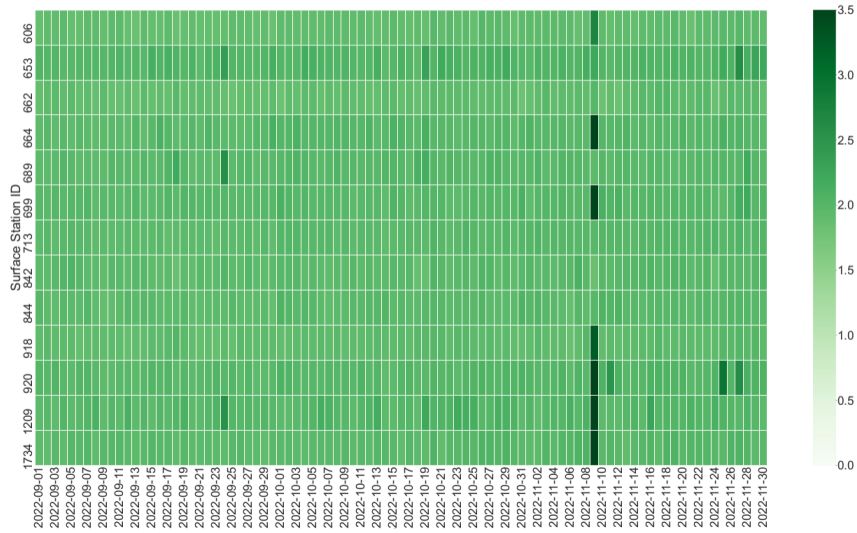
Figure 5: Map of daily mean values of the baseline RMS. Inhomogeneities resulting in darker vertical lines correspond to noise due to lightning storms in the array.

requirements of the electronics. Similarly, the channels used for sPMT and the low-gain of LPMTs (right panel of Fig. 4) and SSDs are well below 1 ADC channel.

In Fig. 5 is shown the evolution of the daily mean baseline RMS expressed in ADC counts for a subsample of detectors in the array during three months. On the vertical scale, station identification numbers are shown. The uniformity in the horizontal lines indicates the stability of the detectors. Furthermore, darker vertical lines due to the presence of lightning storms can be seen during this period; the corresponding days are object of ongoing studies, aiming to identify intervals in the data taking unsuitable for physics analysis. The daily mean value of the MIP charge is shown in Fig. 6 for the same period and the same subsample of stations. Very good stability in time and a general uniformity among stations can be observed. The same was observed for the VEM value.

The distributions of the average VEM and MIP charge values are shown in Fig. 7 for all upgraded detector on an example day of those studied in the maps. They show good agreement
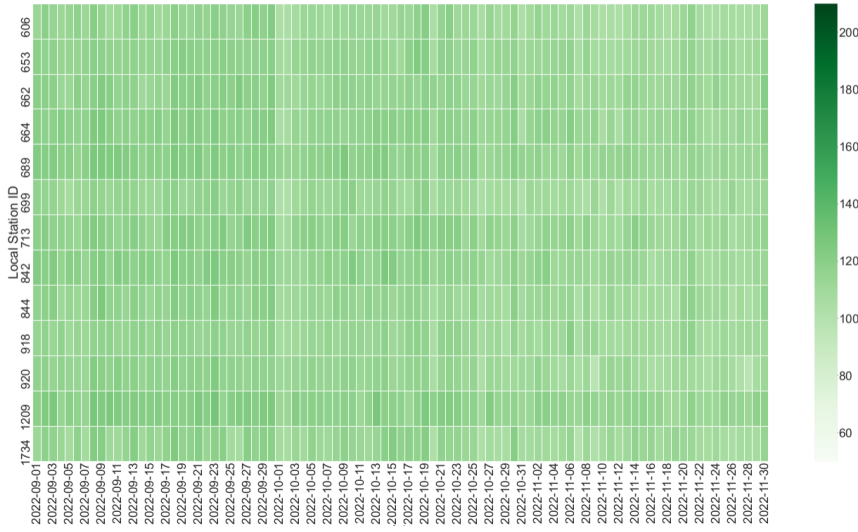
Figure 6: Map of daily mean values of the MIP.
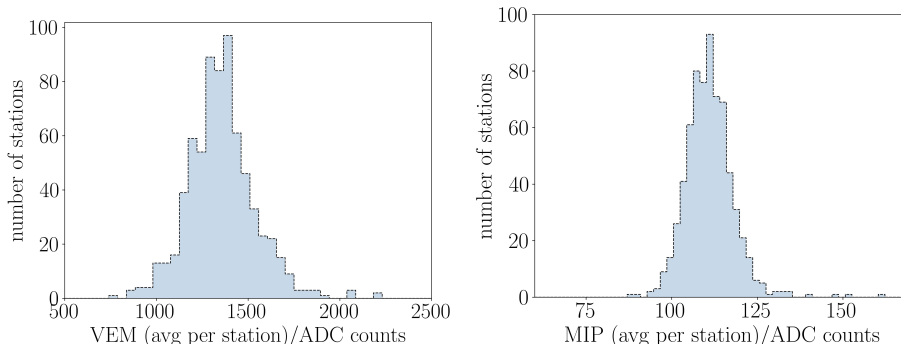
Figure 7: (Left) Distribution of the average VEM values measured in the upgraded array. The distribution shows a mean of 1400±8 ADC counts. (Right) Distribution of the average MIP values measured in the upgraded array. The distribution shows an average value of 110.4±0.2 ADC counts.

and general uniformity among stations of the calibration values in ADC counts evaluated by the electronics. These distributions have remained stable until the end of the deployment with small seasonal fluctuations ≲10% [4] [12] for the two averages values under study.

The cross-calibration factor β is continuously monitored to assess the status of each sPMT. During the deployment, the stability in time of the cross-calibration procedure was verified and the expected trend of the β parameter with temperature has been confirmed. In particular, a yearly evolution in the average of the cross-calibration factor as large as ±10% is observed, due to the seasonal variation of the temperatures in the field. Moreover, a general uniformity over the SD array has been found also for the sPMT cross-calibration, as can be seen in Fig. 8 where the distribution of the average β factor per station is shown for an example day in early July 2023.
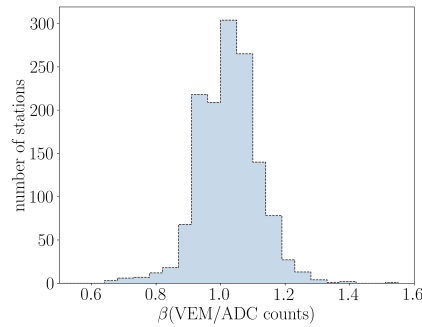
Figure 8: Distribution of the average β factors for all sPMTs in the array in the early July 2023. The distribution shows a mean value of 1.024±0.003 VEM/ADC counts.

5. Summary

AugerPrime involves the introduction of new detectors and upgraded electronics to improve the discrimination of the electromagnetic and muonic components of EAS. The analysis pipeline and monitoring software have been upgraded to analyze the data from the upgraded stations. Currently, the deployment of SSD and UUB is completed, a subset of parameters were continuously monitored to ensure that the design parameters were achieved and that the stations are properly operating throughout the array. The results of the commissioning analysis show that the detectors are performing as expected and good uniformity and long-term stability are obtained.

References

[1] I. Allekotte *et al.*, Nucl. Instrum. Meth. **A** (2007) 409–420.

[2] Ioana C. Mariş *et al.*[Pierre Auger coll.], 32nd International Cosmic Ray Conference **1** (2011) 267–270.

[3] A. Aab *et al.*, [1604.03637] [astro-ph.IM].

[4] G. Cataldi *et al.*[Pierre Auger coll.], Proc. 37th Int. Cosmic Ray Conf., Online – Berlin, Germany, (2021), PoS(ICRC2021)251.

[5] J. Pawlowsky *et al.*[Pierre Auger coll.], PoS(ICRC2023)344.

[6] G. Anastasi *et al.*[Pierre Auger coll.], PoS(ICRC2023)343.

[7] J. de Jesús *et al.*[Pierre Auger coll.], PoS(ICRC2023)267.

[8] D. Nitz *et al.*[Pierre Auger coll.], Proc. 36th Int. Cosmic Ray Conf., Madison (WI), U.S.A. (2019), PoS(ICRC2019)370, [1909.09073].

[9] R. Sato *et al.*[Pierre Auger coll.], PoS(ICRC2023)373.

[10] X. Bertou *et al.*, *Calibration of the surface array of the Pierre Auger Observatory*, Nucl. Instrum. Meth. A **568** (2006) 839–846, [2102.01656].

[11] O. Zapparrata *et al.*[Pierre Auger coll.], PoS(ICRC2023)266.

[12] Z. Zong *et al.*[Pierre Auger coll.], Proc. 35th Int. Cosmic Ray Conf., Busan, South Korea, (2021), PoS(ICRC2017)449.

The Pierre Auger Collaboration

PIERRE AUGER OBSERVATORY

A. Abdul Halim[13], P. Abreu[72], M. Aglietta[54,52], I. Allekotte[1], K. Almeida Cheminant[70], A. Almela[7,12], R. Aloisio[45,46], J. Alvarez-Muñiz[79], J. Ammerman Yebra[79], G.A. Anastasi[54,52], L. Anchordoqui[86], B. Andrada[7], S. Andringa[72], C. Aramo[50], P.R. Araújo Ferreira[42], E. Arnone[63,52], J. C. Arteaga Velázquez[67], H. Asorey[7], P. Assis[72], G. Avila[11], E. Avocone[57,46], A.M. Badescu[75], A. Bakalova[32], A. Balaceanu[73], F. Barbato[45,46], A. Bartz Mocellin[85], J.A. Bellido[13,69], C. Berat[36], M.E. Bertaina[63,52], G. Bhatta[70], M. Bianciotto[63,52], P.L. Biermann[h], V. Binet[5], K. Bismark[39,7], T. Bister[80,81], J. Biteau[37], J. Blazek[32], C. Bleve[36], J. Blümer[41], M. Boháčová[32], D. Boncioli[57,46], C. Bonifazi[8,26], L. Bonneau Arbeletche[21], N. Borodai[70], J. Brack[j], P.G. Brichetto Orchera[7], F.L. Briechle[42], A. Bueno[78], S. Buitink[15], M. Buscemi[47,61], M. Büsken[39,7], A. Bwembya[80,81], K.S. Caballero-Mora[66], S. Cabana-Freire[79], L. Caccianiga[59,49], I. Caracas[38], R. Caruso[58,47], A. Castellina[54,52], F. Catalani[18], G. Cataldi[48], L. Cazon[79], M. Cerda[10], A. Cermenati[45,46], J.A. Chinellato[21], J. Chudoba[32], L. Chytka[33], R.W. Clay[13], A.C. Cobos Cerutti[6], R. Colalillo[60,50], A. Coleman[90], M.R. Coluccia[48], R. Conceição[72], A. Condorelli[37], G. Consolati[49,55], M. Conte[56,48], F. Convenga[41], D. Correia dos Santos[28], P.J. Costa[72], C.E. Covault[84], M. Cristinziani[44], C.S. Cruz Sanchez[3], S. Dasso[4,2], K. Daumiller[41], B.R. Dawson[13], R.M. de Almeida[28], J. de Jesús[7,41], S.J. de Jong[80,81], J.R.T. de Mello Neto[26,27], I. De Mitri[45,46], J. de Oliveira[17], D. de Oliveira Franco[21], F. de Palma[56,48], V. de Souza[19], E. De Vito[56,48], A. Del Popolo[58,47], O. Deligny[34], N. Denner[32], L. Deval[41,7], A. di Matteo[52], M. Dobre[73], C. Dobrigkeit[21], J.C. D'Olivo[68], L.M. Domingues Mendes[72], J.C. dos Anjos, R.C. dos Anjos[25], J. Ebr[32], F. Ellwanger[41], M. Emam[80,81], R. Engel[39,41], I. Epicoco[56,48], M. Erdmann[42], A. Etchegoyen[7,12], C. Evoli[45,46], H. Falcke[80,82,81], J. Farmer[89], G. Farrar[88], A.C. Fauth[21], N. Fazzini[e], F. Feldbusch[40], F. Fenu[41,d], A. Fernandes[72], B. Fick[87], J.M. Figueira[7], A. Filipčič[77,76], T. Fitoussi[41], B. Flaggs[90], T. Fodran[80], T. Fujii[89,f], A. Fuster[7,12], C. Galea[80], C. Galelli[59,49], B. García[6], C. Gaudu[38], H. Gemmeke[40], F. Gesualdi[7,41], A. Gherghel-Lascu[73], P.L. Ghia[34], U. Giaccari[48], M. Giammarchi[49], J. Glombitza[42,g], F. Gobbi[10], F. Gollan[7], G. Golup[1], M. Gómez Berisso[1], P.F. Gómez Vitale[11], J.P. Gongora[11], J.M. González[1], N. González[7], I. Goos[1], D. Góra[70], A. Gorgi[54,52], M. Gottowik[79], T.D. Grubb[13], F. Guarino[60,50], G.P. Guedes[22], E. Guido[44], S. Hahn[39], P. Hamal[32], M.R. Hampel[7], P. Hansen[3], D. Harari[1], V.M. Harvey[13], A. Haungs[41], T. Hebbeker[42], C. Hojvat[e], J.R. Hörandel[80,81], P. Horvath[33], M. Hrabovský[33], T. Huege[41,15], A. Insolia[58,47], P.G. Isar[74], P. Janecek[32], J.A. Johnsen[85], J. Jurysek[32], A. Kääpä[38], K.H. Kampert[38], B. Keilhauer[41], A. Khakurdikar[80], V.V. Kizakke Covilakam[7,41], H.O. Klages[41], M. Kleifges[40], F. Knapp[39], N. Kunka[40], B.L. Lago[16], N. Langner[42], M.A. Leigui de Oliveira[24], Y Lema-Capeans[79], V. Lenok[39], A. Letessier-Selvon[35], I. Lhenry-Yvon[34], D. Lo Presti[58,47], L. Lopes[72], L. Lu[91], Q. Luce[39], J.P. Lundquist[76], A. Machado Payeras[21], M. Majercakova[32], D. Mandat[32], B.C. Manning[13], P. Mantsch[e], S. Marafico[34], F.M. Mariani[59,49], A.G. Mariazzi[3], I.C. Mariş[14], G. Marsella[61,47], D. Martello[56,48], S. Martinelli[41,7], O. Martínez Bravo[64], M.A. Martins[79], M. Mastrodicasa[57,46], H.J. Mathes[41], J. Matthews[a], G. Matthiae[62,51], E. Mayotte[85,38], S. Mayotte[85], P.O. Mazur[e], G. Medina-Tanco[68], J. Meinert[38], D. Melo[7], A. Menshikov[40], C. Merx[41], S. Michal[33], M.I. Micheletti[5], L. Miramonti[59,49], S. Mollerach[1], F. Montanet[36], L. Morejon[38], C. Morello[54,52], A.L. Müller[32], K. Mulrey[80,81], R. Mussa[52], M. Muzio[88], W.M. Namasaka[38], S. Negi[32], L. Nellen[68], K. Nguyen[87], G. Nicora[9], M. Niculescu-Oglinzanu[73], M. Niechciol[44], D. Nitz[87], D. Nosek[31], V. Novotny[31], L. Nožka[33], A Nucita[56,48], L.A. Núñez[30], C. Oliveira[19], M. Palatka[32], J. Pallotta[9], S. Panja[32], G. Parente[79], T. Paulsen[38], J. Pawlowsky[38], M. Pech[32], J. Pękala[70], R. Pelayo[65], L.A.S. Pereira[23], E.E. Pereira Martins[39,7], J. Perez Armand[20], C. Pérez Bertolli[7,41], L. Perrone[56,48], S. Petrera[45,46], C. Petrucci[57,46], T. Pierog[41], M. Pimenta[72], M. Platino[7], B. Pont[80], M. Pothast[81,80], M. Pourmohammad Shahvar[61,47], P. Privitera[89], M. Prouza[32], A. Puyleart[87], S. Querchfeld[38], J. Rautenberg[38], D. Ravignani[7], M. Reininghaus[39], J. Ridky[32], F. Riehn[79], M. Risse[44], V. Rizi[57,46], W. Rodrigues de Carvalho[80], E. Rodriguez[7,41], J. Rodriguez Rojo[11], M.J. Roncoroni[7], S. Rossoni[43], M. Roth[41], E. Roulet[1], A.C. Rovero[4], P. Ruehl[44], A. Saftoiu[73], M. Saharan[80], F. Salamida[57,46], H. Salazar[64], G. Salina[51], J.D. Sanabria Gomez[30], F. Sánchez[7], E.M. Santos[20], E. Santos[32],

9

F. Sarazin[85], R. Sarmento[72], R. Sato[11], P. Savina[91], C.M. Schäfer[41], V. Scherini[56,48], H. Schieler[41], M. Schimassek[34], M. Schimp[38], F. Schlüter[41], D. Schmidt[39], O. Scholten[15,i], H. Schoorlemmer[80,81], P. Schovánek[32], F.G. Schröder[90,41], J. Schulte[42], T. Schulz[41], S.J. Sciutto[3], M. Scornavacche[7,41], A. Segreto[53,47], S. Sehgal[38], S.U. Shivashankara[76], G. Sigl[43], G. Silli[7], O. Sima[73,b], F. Simon[40], R. Smau[73], R. Šmída[89], P. Sommers[k], J.F. Soriano[86], R. Squartini[10], M. Stadelmaier[32], D. Stanca[73], S. Stanič[76], J. Stasielak[70], P. Stassi[36], S. Strähnz[39], M. Straub[42], M. Suárez-Durán[14], T. Suomijärvi[37], A.D. Supanitsky[7], Z. Svozilikova[32], Z. Szadkowski[71], A. Tapia[29], C. Taricco[63,52], C. Timmermans[81,80], O. Tkachenko[41], P. Tobiska[32], C.J. Todero Peixoto[18], B. Tomé[72], Z. Torrès[36], A. Travaini[10], P. Travnicek[32], C. Trimarelli[57,46], M. Tueros[3], M. Unger[41], L. Vaclavek[33], M. Vacula[33], J.F. Valdés Galicia[68], L. Valore[60,50], E. Varela[64], A. Vásquez-Ramírez[30], D. Veberič[41], C. Ventura[27], I.D. Vergara Quispe[3], V. Verzi[51], J. Vicha[32], J. Vink[83], J. Vlastimil[32], S. Vorobiov[76], C. Watanabe[26], A.A. Watson[c], A. Weindl[41], L. Wiencke[85], H. Wilczyński[70], D. Wittkowski[38], B. Wundheiler[7], B. Yue[38], A. Yushkov[32], O. Zapparrata[14], E. Zas[79], D. Zavrtanik[76,77], M. Zavrtanik[77,76]

———— • ————

[1] Centro Atómico Bariloche and Instituto Balseiro (CNEA-UNCuyo-CONICET), San Carlos de Bariloche, Argentina

[2] Departamento de Física and Departamento de Ciencias de la Atmósfera y los Océanos, FCEyN, Universidad de Buenos Aires and CONICET, Buenos Aires, Argentina

[3] IFLP, Universidad Nacional de La Plata and CONICET, La Plata, Argentina

[4] Instituto de Astronomía y Física del Espacio (IAFE, CONICET-UBA), Buenos Aires, Argentina

[5] Instituto de Física de Rosario (IFIR) – CONICET/U.N.R. and Facultad de Ciencias Bioquímicas y Farmacéuticas U.N.R., Rosario, Argentina

[6] Instituto de Tecnologías en Detección y Astropartículas (CNEA, CONICET, UNSAM), and Universidad Tecnológica Nacional – Facultad Regional Mendoza (CONICET/CNEA), Mendoza, Argentina

[7] Instituto de Tecnologías en Detección y Astropartículas (CNEA, CONICET, UNSAM), Buenos Aires, Argentina

[8] International Center of Advanced Studies and Instituto de Ciencias Físicas, ECyT-UNSAM and CONICET, Campus Miguelete – San Martín, Buenos Aires, Argentina

[9] Laboratorio Atmósfera – Departamento de Investigaciones en Láseres y sus Aplicaciones – UNIDEF (CITEDEF-CONICET), Argentina

[10] Observatorio Pierre Auger, Malargüe, Argentina

[11] Observatorio Pierre Auger and Comisión Nacional de Energía Atómica, Malargüe, Argentina

[12] Universidad Tecnológica Nacional – Facultad Regional Buenos Aires, Buenos Aires, Argentina

[13] University of Adelaide, Adelaide, S.A., Australia

[14] Université Libre de Bruxelles (ULB), Brussels, Belgium

[15] Vrije Universiteit Brussels, Brussels, Belgium

[16] Centro Federal de Educação Tecnológica Celso Suckow da Fonseca, Petropolis, Brazil

[17] Instituto Federal de Educação, Ciência e Tecnologia do Rio de Janeiro (IFRJ), Brazil

[18] Universidade de São Paulo, Escola de Engenharia de Lorena, Lorena, SP, Brazil

[19] Universidade de São Paulo, Instituto de Física de São Carlos, São Carlos, SP, Brazil

[20] Universidade de São Paulo, Instituto de Física, São Paulo, SP, Brazil

[21] Universidade Estadual de Campinas, IFGW, Campinas, SP, Brazil

[22] Universidade Estadual de Feira de Santana, Feira de Santana, Brazil

[23] Universidade Federal de Campina Grande, Centro de Ciencias e Tecnologia, Campina Grande, Brazil

[24] Universidade Federal do ABC, Santo André, SP, Brazil

[25] Universidade Federal do Paraná, Setor Palotina, Palotina, Brazil

[26] Universidade Federal do Rio de Janeiro, Instituto de Física, Rio de Janeiro, RJ, Brazil

[27] Universidade Federal do Rio de Janeiro (UFRJ), Observatório do Valongo, Rio de Janeiro, RJ, Brazil

[28] Universidade Federal Fluminense, EEIMVR, Volta Redonda, RJ, Brazil

[29] Universidad de Medellín, Medellín, Colombia

[30] Universidad Industrial de Santander, Bucaramanga, Colombia

[31] Charles University, Faculty of Mathematics and Physics, Institute of Particle and Nuclear Physics, Prague, Czech Republic

[32] Institute of Physics of the Czech Academy of Sciences, Prague, Czech Republic

[33] Palacky University, Olomouc, Czech Republic

[34] CNRS/IN2P3, IJCLab, Université Paris-Saclay, Orsay, France

[35] Laboratoire de Physique Nucléaire et de Hautes Energies (LPNHE), Sorbonne Université, Université de Paris, CNRS-IN2P3, Paris, France

[36] Univ. Grenoble Alpes, CNRS, Grenoble Institute of Engineering Univ. Grenoble Alpes, LPSC-IN2P3, 38000 Grenoble, France

[37] Université Paris-Saclay, CNRS/IN2P3, IJCLab, Orsay, France

[38] Bergische Universität Wuppertal, Department of Physics, Wuppertal, Germany

[39] Karlsruhe Institute of Technology (KIT), Institute for Experimental Particle Physics, Karlsruhe, Germany

[40] Karlsruhe Institute of Technology (KIT), Institut für Prozessdatenverarbeitung und Elektronik, Karlsruhe, Germany

[41] Karlsruhe Institute of Technology (KIT), Institute for Astroparticle Physics, Karlsruhe, Germany

[42] RWTH Aachen University, III. Physikalisches Institut A, Aachen, Germany

[43] Universität Hamburg, II. Institut für Theoretische Physik, Hamburg, Germany

[44] Universität Siegen, Department Physik – Experimentelle Teilchenphysik, Siegen, Germany

[45] Gran Sasso Science Institute, L'Aquila, Italy

[46] INFN Laboratori Nazionali del Gran Sasso, Assergi (L'Aquila), Italy

[47] INFN, Sezione di Catania, Catania, Italy

[48] INFN, Sezione di Lecce, Lecce, Italy

[49] INFN, Sezione di Milano, Milano, Italy

[50] INFN, Sezione di Napoli, Napoli, Italy

[51] INFN, Sezione di Roma "Tor Vergata", Roma, Italy

[52] INFN, Sezione di Torino, Torino, Italy

[53] Istituto di Astrofisica Spaziale e Fisica Cosmica di Palermo (INAF), Palermo, Italy

[54] Osservatorio Astrofisico di Torino (INAF), Torino, Italy

[55] Politecnico di Milano, Dipartimento di Scienze e Tecnologie Aerospaziali , Milano, Italy

[56] Università del Salento, Dipartimento di Matematica e Fisica "E. De Giorgi", Lecce, Italy

[57] Università dell'Aquila, Dipartimento di Scienze Fisiche e Chimiche, L'Aquila, Italy

[58] Università di Catania, Dipartimento di Fisica e Astronomia "Ettore Majorana", Catania, Italy

[59] Università di Milano, Dipartimento di Fisica, Milano, Italy

[60] Università di Napoli "Federico II", Dipartimento di Fisica "Ettore Pancini", Napoli, Italy

[61] Università di Palermo, Dipartimento di Fisica e Chimica "E. Segrè", Palermo, Italy

[62] Università di Roma "Tor Vergata", Dipartimento di Fisica, Roma, Italy

[63] Università Torino, Dipartimento di Fisica, Torino, Italy

[64] Benemérita Universidad Autónoma de Puebla, Puebla, México

[65] Unidad Profesional Interdisciplinaria en Ingeniería y Tecnologías Avanzadas del Instituto Politécnico Nacional (UPIITA-IPN), México, D.F., México

[66] Universidad Autónoma de Chiapas, Tuxtla Gutiérrez, Chiapas, México

[67] Universidad Michoacana de San Nicolás de Hidalgo, Morelia, Michoacán, México

[68] Universidad Nacional Autónoma de México, México, D.F., México

[69] Universidad Nacional de San Agustin de Arequipa, Facultad de Ciencias Naturales y Formales, Arequipa, Peru

[70] Institute of Nuclear Physics PAN, Krakow, Poland

[71] University of Łódź, Faculty of High-Energy Astrophysics,Łódź, Poland

[72] Laboratório de Instrumentação e Física Experimental de Partículas – LIP and Instituto Superior Técnico – IST, Universidade de Lisboa – UL, Lisboa, Portugal

[73] "Horia Hulubei" National Institute for Physics and Nuclear Engineering, Bucharest-Magurele, Romania

[74] Institute of Space Science, Bucharest-Magurele, Romania

[75] University Politehnica of Bucharest, Bucharest, Romania

[76] Center for Astrophysics and Cosmology (CAC), University of Nova Gorica, Nova Gorica, Slovenia

[77] Experimental Particle Physics Department, J. Stefan Institute, Ljubljana, Slovenia

[78] Universidad de Granada and C.A.F.P.E., Granada, Spain

[79] Instituto Galego de Física de Altas Enerxías (IGFAE), Universidade de Santiago de Compostela, Santiago de Compostela, Spain

[80] IMAPP, Radboud University Nijmegen, Nijmegen, The Netherlands

[81] Nationaal Instituut voor Kernfysica en Hoge Energie Fysica (NIKHEF), Science Park, Amsterdam, The Netherlands

[82] Stichting Astronomisch Onderzoek in Nederland (ASTRON), Dwingeloo, The Netherlands

[83] Universiteit van Amsterdam, Faculty of Science, Amsterdam, The Netherlands

[84] Case Western Reserve University, Cleveland, OH, USA

[85] Colorado School of Mines, Golden, CO, USA

[86] Department of Physics and Astronomy, Lehman College, City University of New York, Bronx, NY, USA

[87] Michigan Technological University, Houghton, MI, USA

[88] New York University, New York, NY, USA

[89] University of Chicago, Enrico Fermi Institute, Chicago, IL, USA

[90] University of Delaware, Department of Physics and Astronomy, Bartol Research Institute, Newark, DE, USA

[91] University of Wisconsin-Madison, Department of Physics and WIPAC, Madison, WI, USA

——

[a] Louisiana State University, Baton Rouge, LA, USA

[b] also at University of Bucharest, Physics Department, Bucharest, Romania

[c] School of Physics and Astronomy, University of Leeds, Leeds, United Kingdom

[d] now at Agenzia Spaziale Italiana (ASI). Via del Politecnico 00133, Roma, Italy

[e] Fermi National Accelerator Laboratory, Fermilab, Batavia, IL, USA

[f] now at Graduate School of Science, Osaka Metropolitan University, Osaka, Japan

[g] now at ECAP, Erlangen, Germany

[h] Max-Planck-Institut für Radioastronomie, Bonn, Germany

[i] also at Kapteyn Institute, University of Groningen, Groningen, The Netherlands

[j] Colorado State University, Fort Collins, CO, USA

[k] Pennsylvania State University, University Park, PA, USA

Acknowledgments